Secondary Structure and Stability of the Bacterial Carbohydrate-Specific Recognition Proteins K88ab, AFA-1, NFA-1, and CFA-1

Rainer Knörle and Wigand Hübner*

Institut für Physikalische Chemie, Universität Freiburg, Albertstrasse 23 a, D-79104 Freiburg, Germany

Received February 1, 1995; Revised Manuscript Received June 13, 1995[⊗]

ABSTRACT: The conformation and thermodynamic stability of the four polymeric carbohydrate-specific bacterial recognition proteins K88ab, AFA-1, NFA-1, and CFA-1 and their monomeric subunits that can be obtained by variation of pH were studied by infrared spectroscopy and differential scanning microcalorimetry. For NFA-1, a pH-dependent dissociation of the polymeric form cannot be achieved due to the stronger interactions of the neighboring subunits. Generally, no alterations in secondary structure are observed between the monomeric and the polymeric proteins. All adhesins reveal a high degree of β-sheet structure (40−55%), while the α-helix component is of minor importance (10−20%). The adhesins investigated in this study revealed unusually high denaturation temperatures (69−104 °C) and stabilizing Gibbs energies, ΔG (40−125 kJ/mol), compared to common globular proteins. Statistical deconvolution of the DSC curves yields a two-state transition of K88ab, NFA-1, and the monomeric CFA-1 and the existence of intermediate states for AFA-1 and polymeric CFA-1 during the denaturation process. The irreversible denaturation of K88ab, AFA-1, and CFA-1 is explained by aggregation of the polypeptide chains forming a three-dimensional network of intermolecular β-sheet-type structures. In contrast, denaturation of NFA-1 is completely reversible. At a physiologically relevant temperature of ~40 °C, we observe predenaturational events in the DSC curves of polymeric K88ab and NFA-1 with no concomittant changes in the secondary structure of these proteins.

The adherence of pathogenic bacteria to epithelial surfaces represents an important early event in the interaction of these bacteria with the host that leads to colonization and infection. Adhesion is mediated by carbohydrate-specific bacterial recognition proteins, the adhesins. Adhesive bacteria frequently show proteinaceous fibrillar structures on their surface which are distinct from the sex pili and from the flagella and have been termed fimbriae or pili (Duguid et al., 1955). Other bacteria are adhesive without presenting electron microscopically recognizable fimbriae. Thus, adhesins are commonly classified as fimbrial and nonfimbrial (Jann & Hoschützky, 1990).

Swine pathogenic *Escherichia coli* exhibit the K88 antigen, a fimbrial adhesin 2−3 nm in diameter consisting of identical adhesive 27.5-kDa subunits (Klemm, 1981). The afimbrial adhesin AFA-1 composed of a single repeating 16-kDa subunit is expressed by a human pyelonephritic *E. coli* strain (Labigne-Roussel et al., 1985). Enterotoxigenic *E. coli* strains responsible for severe diarrhea in man mediate their specific adherence to the human intestinal mucosa by the fimbrial colonization factor antigen CFA-1 consisting of ~100 identical adhesive subunits (Evans et al., 1975). The degree of aggregation of these adhesins held together by hydrophobic interactions may be influenced by variation of pH. In contrast, the nonfimbrial adhesin NFA-1 expressed by *E. coli* 827, a strain causing urinary tract infections and sepsis, cannot be disintegrated into its native monomeric subunits. This protein, forming an amorphous capsule-like aggregate around the bacterium, consists of 150−440 identical 16-kDa subunits (Jann & Hoschützky, 1990) which are held together by intermolecular hydrogen bonds (Ahrends, 1991).

Though the origins of these four representative fimbrial and nonfimbrial adhesins are quite different, the similarities in their molecular arrangements and sizes, e.g. aggregation of 100−500 identical subunits into a chainlike polymeric form with a molecular weight of several million, and the possibility to obtain and investigate the monomeric subunits justify a common treatment.

The aim of this study is to deduce the thermodynamic profile of the polymeric adhesins and to compare these results with the thermodynamic data obtained from differential scanning calorimetry experiments of the monomeric subunits. In addition, we used infrared spectroscopy to detect differences between the monomeric and polymeric adhesins on a molecular level. This method is widely used for the analysis of protein secondary structure (Surewicz & Mantsch, 1988; Dousseau & Pézolet, 1990; Lee et al., 1990; Surewicz et al., 1987; Singh et al., 1990; Jackson et al., 1991) or of structural alterations of proteins and glycoproteins caused by denaturation (Clark et al., 1981; Kato et al., 1987) or disease (Knörle et al., 1994; Fabian et al., 1993), although it has been critically assessed by Surewicz et al. (1993).

In contrast to other methods for the analysis of protein secondary structure like X-ray analysis, circular dichroism studies, or NMR experiments, FTIR spectroscopy is especially suitable for the investigation of the secondary structure of the polymeric and amorphous bacterial adhesins. Due to the long wavelength of infrared light, scattering of the incident light at the investigated polymeric protein aggregates, which renders circular dichroism measurements most difficult, does not occur. On account of the high molecular weight of the adhesins, X-ray crystallography and

* Author for correspondence. Fax: +49-761-203 6189.

[⊗] Abstract published in *Advance ACS Abstracts,* August 15, 1995.

0006-2960/95/0434-10970$09.00/0

NMR spectroscopic experiments are not possible. Another advantage of the FTIR technique is the possibility of recording spectra at different temperatures, thus allowing an investigation of the protein denaturation process.

MATERIALS AND METHODS

Preparation of Adhesins. Prior to cultivation, the bacterial strains *E. coli* D 250 (K88ab), *E. coli* KS 52 (AFA-1), *E. coli* 827 (NFA-1), and *E. coli* H10407 (CFA-1) were selected for their ability to agglutinate human erythrocytes. The bacteria were grown on Loeb agar (Loeb & Zidner, 1961) or CFA agar (Evans et al., 1977) at 37 °C for at least 18 h. After the bacteria were harvested in a buffer containing 75 mM NaCl and 75 mM sodium phosphate, pH 7.5, this suspension was agitated six times for 5 min with an Omnimixer (Sorvall, Newton, setting 3) under cooling in an ice bath. The bacteria were removed after centrifugation (16000*g*, 30 min, 5 °C) as a pellet. The adhesins were precipitated from the supernatant with ammonium sulfate (40% saturation at pH 8 and 4 °C). The precipitated protein was collected by centrifugation (14000*g*, 30 min, 5 °C), and the pellet was suspended in and dialyzed against 10 mM Tris/HCl, pH 7.5. Insoluble material was removed by centrifugation (10000*g*, 60 min). To remove contaminating lipopolysaccharide, the supernatant was applied to a column of Fractogel EMD TMAE-650 (M) (Merck, Darmstadt, Germany). After the column was washed with 10 mM Tris/HCl pH 8.0, the protein was eluted with a linear concentration gradient from 0 to 50 mM sodium citrate. Fractions were assayed for protein content and purity by SDS–polyacrylamide gel electrophoresis. The adhesin was recovered from the pooled fractions by ammonium sulfate precipitation. After centrifugation (14000*g*, 30 min, 5 °C), the pellet was dissolved in deionized water, dialyzed against 5 mM ammonium bicarbonate, and lyophilized. Prior to utilization, the protein was dissolved in 10 mM Tris/HCl, pH 8.5, and extensively dialyzed against the appropriate buffer. The concentration of protein in solution was determined by means of the BCA assay (Smith et al., 1985) or spectrophotometrically at 25 °C, using calculated extinction coefficients (Gill & von Hippel, 1989).

Differential Scanning Calorimetry (DSC). For DSC experiments a DASM-4 microcalorimeter (V/O Mashpriborintorg, Russia) (Privalov, 1980) was used. In each experiment the temperature was scanned from 20 to 100 or 110 °C at a rate of 1 °C/min. Data points were collected by means of a serial input–output system developed in our laboratory.

The model-independent ΔH_{cal}, ΔS, and ΔG values were obtained directly from the DSC experiments; the error in ΔH is ±5%. Because the denaturation process can be described as a equilibrium between two thermodynamic states, one being stable below and the other above the transition temperature, the ratio

$$\sigma = \Delta H_{cal} I \Delta H_{vH} \quad (1)$$

is used to decide whether the denaturation of a protein follows this two-state model or represents a multistate transition. The model dependent van't Hoff transition enthalpy, ΔH_{vH}, can be derived from DSC plots by means of the equation

$$\Delta H_{vH}(T_m) = 4RT_m^2 \frac{\Delta C_p}{Q_d} \quad (2)$$

where T_m represents the transition temperature and Q_d is the total heat of denaturation (Privalov, 1979). If the process considered is of a two-state transition type, σ should be close to unity. Multistate transitions lead to values of $\sigma > 1$; in cases of intermolecular interactions, σ becomes <1. The average cooperative length N_0, i.e., the number of segments that cooperatively transform to the denatured state, can be calculated according to

$$N_0 = \frac{1}{\sigma} \quad (3)$$

Besides the criterion of the σ parameter, the validity of the two-state model for the denaturation of proteins can be studied using statistical thermodynamics (Freire & Biltonen, 1978). Application of this deconvolution procedure to DSC data allows the determination of the fraction of molecules occupying intermediate states during denaturation.

FTIR Spectroscopy. Spectra were recorded at a resolution of 2 cm^{-1} using a Bruker IFS 113v Fourier transform infrared spectrometer equipped with an MCT detector. For H/D exchange the protein–buffer solutions were lyophylized, dissolved three times in deuterium oxide (99.8 atom %, Sigma Chemicals), and lyophylized again. A good H/D exchange was monitored by the absence of the O–H stretching vibration at ~3600 cm^{-1} and the shift of the amide II′ band. Probes (5%, w/v) were placed in a cell fitted with CaF_2 windows and a 50-μm PTFE spacer. The temperature of the sample was controlled by means of a cell jacket of circulating water. Temperature was measured via a thermocouple placed against the cell window. The spectrometer was continuously purged with dry air to avoid water vapor interference. A total of 512 interferograms were collected, apodized, and Fourier transformed. Buffer and sample spectra were recorded under the same temperature and scanning conditions.

Fourier self-deconvolution and assignment of the bands to secondary structure elements was carried out according to Byler and Susi (1986). The application of factor analysis followed the method described by Lee et al. (1990) and the algorithm presented by Fredericks et al. (1985). The calibration set used in our study consisted of spectra recorded in deuterium oxide at 25 °C of the following globular proteins whose secondary structures were determined by X-ray analysis: myoglobin, hemoglobin, triose-phosphate isomerase, cytochrome *c*, lysozyme, alcohol dehydrogenase, papain, trypsin inhibitor, ribonuclease A, ribonuclease S, trypsinogen, carbonic anhydrase, chymotrypsinogen A, pepsin, chymotrypsin, elastase, prealbumin, and concanavalin A. Secondary structures were assigned according to Levitt and Greer (1977). Spectra were based line corrected between 1700 and 1600 cm^{-1}, and the integral intensity of all spectra was adjusted to a common value. Seven factors were retained in the data set, and the seven factor loadings were used in the multiple linear regression in the calibration step. We found that this number of factors (loadings) gave the best prediction for the secondary structure content, percent α-helix and percent β-sheet. For this purpose each of the 18 proteins was eliminated from the calibration set, and its "unknown" properties of interest were predicted by the remaining 17

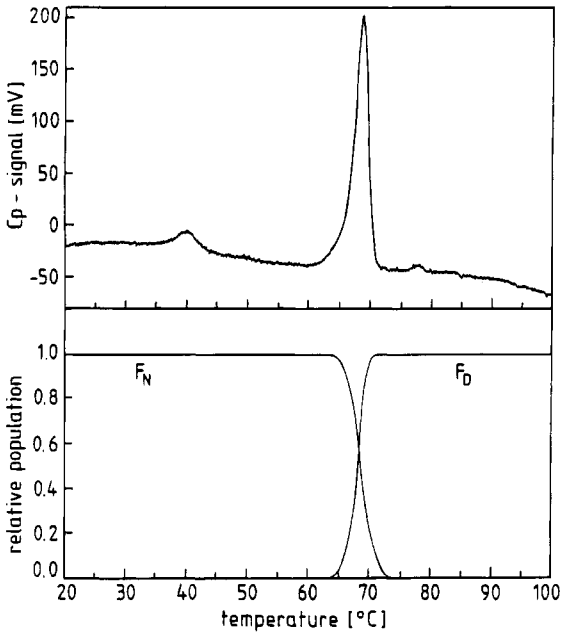

FIGURE 1: (Top) DSC transition curve of K88ab in 10 mM Tris/HCl, pH 8.5. Protein concentration was 1.25 mg/mL. (Bottom) Plot of the relative populations of the states present in the denaturation process obtained by statistical deconvolution of the DSC profile. F_N represents the native state; F_D, the denatured state.

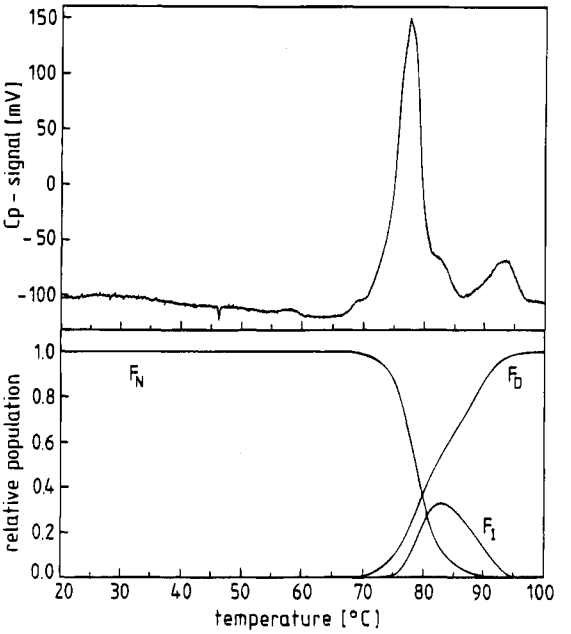

FIGURE 2: (Top) DSC transition curve of AFA-1 in 10 mM Tris/HCl, pH 8.5. Protein concentration was 1.78 mg/mL. (Bottom) Plot of the relative populations of the states present in the denaturation process obtained by statistical deconvolution of the DSC profile. F_N represents the native state; F_I, the intermediate; and F_D, the denatured state.

proteins in the calibration set. The standard error of prediction (SEP) was calculated according to

$$\mathrm{SEP} = \sqrt{\frac{\sum_{j}^{n}(p_{f_j} - p_{x_j})^2}{n}} \qquad (4)$$

where p_{f_j} is the proportion of structure predicted by factor analysis in protein j, p_{x_j} is the proportion of structure calculated from the original X-ray data for protein j, and n is the number of proteins. The SEP values (in % structure) obtained were 9.2 for α-helix and 6.5 for β-sheet. The suitability of the method was additionally evaluated via the correlation coefficients r generated by linear regression of the predicted and true values of each property in the calibration set. This resulted in values of r (α-helix) = 0.89 and r (β-sheet) = 0.86.

RESULTS AND DISCUSSION

DSC Experiments. The degree of aggregation of the bacterial adhesins K88ab, AFA-1, and CFA-1 can be influenced by variation of pH. These proteins, existing in a polymeric form at lower pH held together by hydrophobic interactions, disintegrate at pH > 7 into a mixture of oligomers. This phenomen explains the specific adherence of the bacteria to the host epithelial surfaces, only the polymeric form of the adhesin mediates adhesion of the bacterium. The monomeric adhesin, existing at higher pH, binds to its receptor without mediating contact to the bacterium. In contrast, the nonfimbrial adhesin NFA-1 only exists in a polymeric form. DSC profiles of the thermal denaturation of K88ab and AFA-1 subunits are shown in the top traces of Figures 1 and 2. The denaturation process of K88ab, AFA-1, and CFA-1 is followed by an irreversible

Table 1: Thermodynamic Parameters for Denaturation of Various Aggregates of Adhesins K88ab, AFA-1, NFA-1, and CFA-1

	pH	T_m (°C)	$-\Delta H_{cal}$ (kJ/mol)	$-\Delta H_{vH}$ (kJ/mol)	σ	N_0	$-\Delta G$ (kJ/mol)
K88ab	6.0	42.4	44	742	0.06	17	2
		69.2	898	1327	0.68	1.5	116
	8.5	40.6	57	677	0.08	12	3
		69.2	958	1236	0.77	1.3	124
AFA-1	6.0	77.5	366	715	0.51	2.0	55
		93.6	53	815	0.07	14	10
	8.5	78.3	399	767	0.52	1.9	60
		93.3	52	829	0.06	17	10
NFA-1	6.0	45.2	36	465	0.08	13	2
		86.7	217	889	0.24	4	37
	8.5	45.6	99	357	0.28	4	6
		86.7	233	925	0.25	4	40
CFA-1	6.0	90.9	79	640	0.11	9.1	14
		103.8	266	585	0.45	2.2	64
	8.5	89.1	535	975	0.55	1.8	97

step as is shown by a repeated heating of the solutions, which leads to only slight deflections of the C_p values from the calorimetric base line. In contrast, the denaturation of NFA-1 proved to be completely reversible. Except for CFA-1, variation of pH and therefore the degree of aggregation leads to no changes in the DSC profiles. While the monomeric CFA-1 shows one irreversible transition, the heat capacity curve of the polymeric form reveals two distinct transitions. The denaturation temperatures, ranging from 69 °C for K88ab up to 104 °C for CFA-1, are unexpectedly high values for proteins. Similar high denaturation temperatures are only known for proteins of extremophilic bacteria (Jaenicke, 1988). The thermodynamic parameters obtained by analysis of the DSC transition curves of the monomeric and polymeric adhesins are listed in Table 1.

As a common feature, the adhesins reveal relatively high values for the stabilizing Gibbs energy compared to other globular proteins. Especially in the case of K88ab, ΔG

values are substantially larger than those obtained for common globular proteins, which usually exhibit Gibbs energies of -50 ± 20 kJ/mol, not depending on their molecular weight (Privalov & Kechinashvili, 1974). This energy, being of a similar order as the $R \times T$ thermal energy, is achieved in various ways; it results as a balance of two large values for the energies of stabilization and repulsion. The large values of the stabilizing Gibbs energies of the adhesins together with their high denaturation temperatures can be regarded as a manifestation of the adaption of these extracellular proteins to their extreme environmental conditions caused by the defensive system of the host.

In contrast to AFA-1 and CFA-1, K88ab and NFA-1 reveal a predenaturational transition occurring in the physiological temperature range of ~40 °C. In both cases, this transition, showing a small enthalpic effect, reveals significant differences between ΔH_{cal} and ΔH_{vH}. This pretransition may be of some biochemical importance. Predenaturational changes are known for several globular proteins (Atanasow et al., 1968; Matheson et al., 1977; Kim & Lumry, 1971) if aggregates of these proteins are present in solution. Therefore, fluctuations of the subunits in the polymeric adhesin may be considered as a reason for this transition. This conjecture is supported by the significant dependence of the cooperative length N_0 on pH, resulting probably from stronger interactions of the subunits at lower pH, the physiological conditions of the uropathogenic bacteria. Because N_0 cannot be larger than the total segment length, fluctuations of the solution structure caused by interactions between solvent and proteins as well as between the proteins themselves may be considered additionally at least in the case of the oligomeric K88ab pretransition.

The denaturational transition of K88ab at 69 °C only shows slight deflections of the cooperativity parameter from unity. These mainly result from the irreversibility of the denaturation process which causes values of $\sigma < 1$ due to the asymmetry of the DSC peak (Privalov, 1979). Deconvolution of the DSC curves, one example of which is given in Figure 1, reveals no intermediates present in the denaturation process, proving the validity of the two-state model for this transition. In the case of NFA-1 with an average cooperative length of 4 during denaturation, deconvolution also revealed no intermediates. During denaturation of AFA-1, an intermediate is formed (Figure 2). According to N_0 showing values of 2, this intermediate can be characterized as the dimeric form of the protein. Deconvolution of the DSC profile of monomeric CFA-1 revealed no intermediates, while during the denaturation of polymeric CFA-1, formation of intermediates occurs.

FTIR Experiments. (A) Secondary Structure. Figure 3 shows the buffer-subtracted infrared spectra of the adhesins recorded in 10 mM Tris/DCl, pD 8.5. Secondary structure contents of these proteins obtained by curve-fitting to deconvoluted spectra and factor analysis are listed in Table 2. Both methods reveal no alteration of the overall secondary structure with a change of pD and therefore of the degree of aggregation of the adhesins K88ab, AFA-1, and CFA-1. In the case of NFA-1, the subunits cannot be obtained by variation of pH; only the rise of temperature above the denaturation temperature leads to disintegration into denatured monomeric subunits (Ahrends, 1991). Therefore, a structural analysis of the native monomeric subunits is not possible.

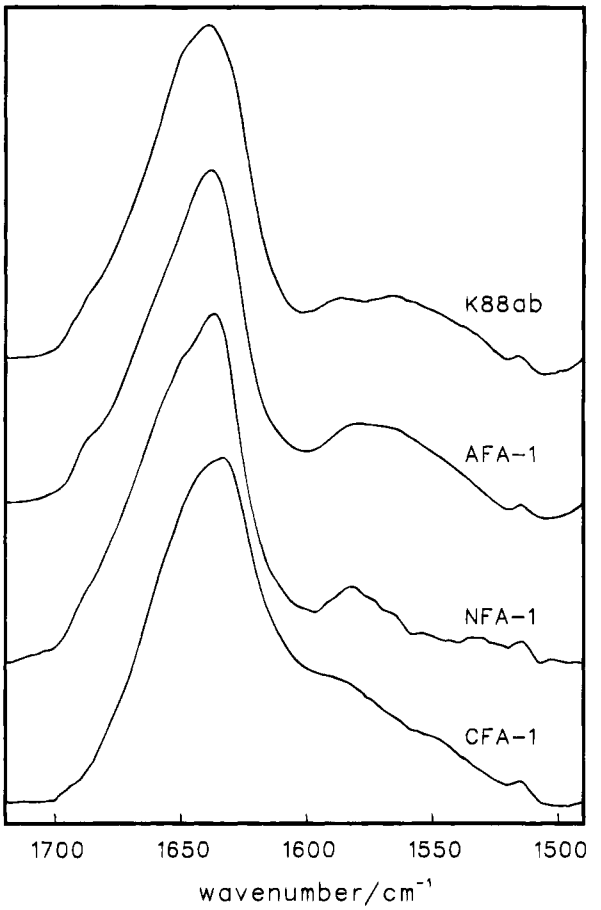

FIGURE 3: Infrared spectra in the amide I′ region of K88ab, AFA-1, NFA-1, and CFA-1 in 10 mM Tris/DCl, pD 8.5, at 20 °C.

Table 2: Secondary Structure Obtained by Analysis of the Amide I′ Band Using Curve Fitting and Factor Analysis

	pH		curve fitting	factor analysis
K88ab	6.0	% α-helix	20	20
		% β-sheet	42	48
	8.5	% α-helix	22	19
		% β-sheet	34	46
AFA-1	6.0	% α-helix	21	18
		% β-sheet	55	47
	8.5	% α-helix	23	15
		% β-sheet	45	48
NFA-1	6.0	% α-helix	12	1
		% β-sheet	50	57
CFA-1	6.0	% α-helix	20	16
		% β-sheet	38	37
	8.5	% α-helix	17	22
		% β-sheet	37	35

The analysis of the secondary structure by means of FTIR spectroscopy reveals a relatively high degree of β-sheet structures (37−57%) in the monomeric subunits of K88ab, AFA-1, and CFA-1. Upon aggregation the high proportion of β-sheet structure and the low α-helical content do not change. For NFA-1, the secondary structure of the polymeric nonfimbrial aggregate also reveals a high degree of β-sheets. A common feature of adhesive proteins, e.g., the bacterial carbohydrate-specific recognition proteins studied in this paper or the class of lectins or the antigen-binding domains of the immunoglobulins, seems to be the high content of β-sheet structures.

(B) Denaturation. Thermal denaturation of proteins represents an unfolding of the ordered configuration of the

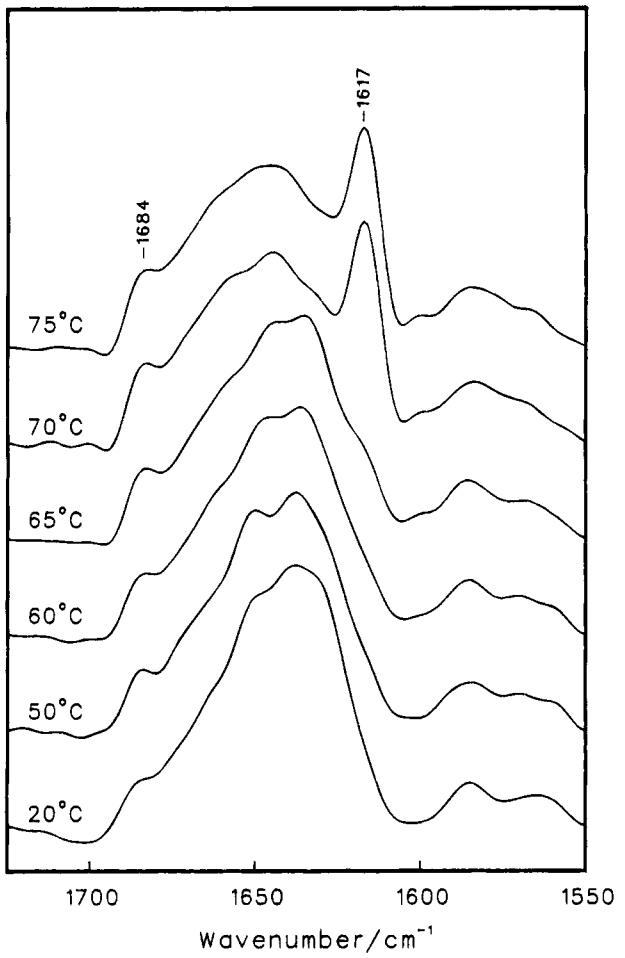

FIGURE 4: Temperature dependence of the infrared spectrum in the amide I′ region of the K88ab subunit. All spectra were subjected to Fourier deconvolution using a Lorentzian line shape of 15 cm^{-1} half-width and a resolution enhancement factor (k value) of 2.

polypeptide chain toward a more disordered spatial distribution. To follow these secondary structure changes during the denaturational process of the adhesins, FTIR spectra of the solutions in D_2O were recorded for different temperatures. The temperatures were chosen according to the calorimetric heat capacity curves. pD values and salt concentrations were the same as in the DSC experiments.

Figure 4 shows deconvoluted spectra of monomeric K88ab recorded at temperatures relevant for the denaturation process. No differences exist between these spectra and the spectra recorded in order to investigate the denaturational behavior of the polymeric form. The first calorimetrically observed transition at ~40 °C leads to no changes in the overall secondary structure as obtained by curve-fitting and factor analysis. The main difference between the spectra recorded at 20 and 50 °C consists in smaller half-widths at half-heights in the 50 °C spectrum. The denaturational transition at 69 °C results in a drastic change in the infrared spectrum. While the intensities of the "component bands", which we assigned to secondary structure elements according to Byler and Susi (1986), decrease, two new bands appear at 1617 and 1683 cm^{-1}. These must be assigned to intermolecular H-bonds (Clark et al., 1981), which lead to the formation of a three-dimensional network. Because secondary structure elements are present even in the spectrum of the totally denatured protein, the network formed has to

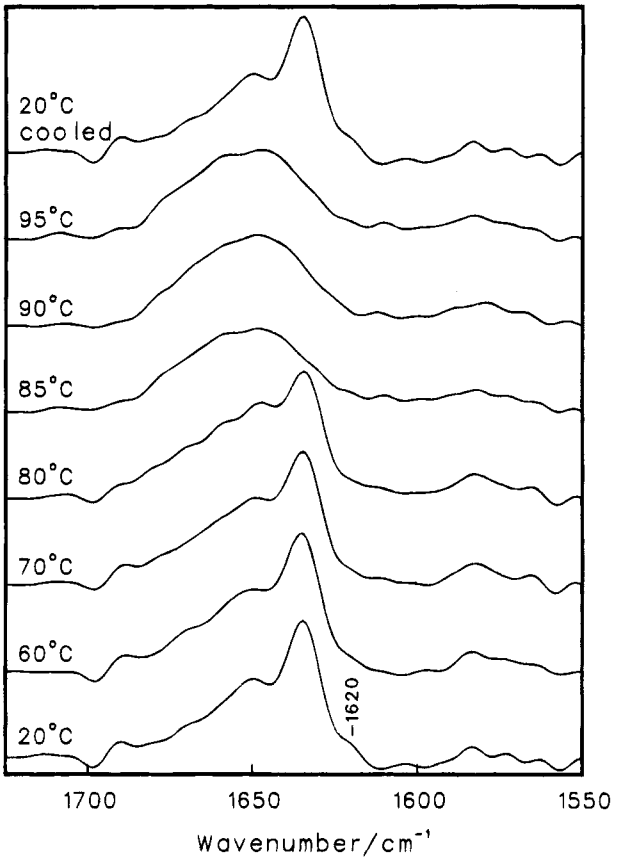

FIGURE 5: Temperature dependence of the infrared spectrum in the amide I′ region of NFA-1. Spectra were subjected to Fourier deconvolution. The top trace represents the amide I′ band measured at 20 °C after cooling of the protein solution from 95 °C.

be described as composed of partially folded globular particles linked together by hydrogen bonds. The bands resulting from these intermolecular H-bonds are little changed on cooling the gel back to 20 °C. Therefore, this spectral feature is indicative of the irreversible denaturation of proteins caused by aggregation of the unfolded polypeptide chains.

Due to the high second transition temperatures of AFA-1 and CFA-1, a complete FTIR investigation of their denaturational process is not possible. Similar to K88ab, both proteins show the appearance of two bands at 1684 and 1617 cm^{-1} in the spectra recorded at 90 °C, which clearly indicate the irreversibility of the denaturation process. But the different thermodynamic behavior of monomeric and polymeric CFA-1 also appears in the infrared spectra. While the monomeric CFA-1 fimbrillin shows the typical formation of the denaturation bands, the structural change of polymeric CFA-1 at 90 °C results in an increased content of unordered structures, resulting from a partial unfolding of the polypeptide chain. The second irreversible transition leading to the total disruption of the native state cannot be followed spectroscopically due to the extremely high denaturation temperature of 104 °C.

The deconvoluted spectra recorded from solutions of NFA-1 at different temperatures are shown in Figure 5. Similar to K88ab, the predenaturational transition leads to no changes in the overall secondary structure. Nevertheless, as may be seen by a comparison of the 20 and 60 °C spectra, the intensity of the shoulder at 1620 cm^{-1}, a band only detected for NFA-1 and not for the other adhesins, decreases.

Due to the spectral region, this band can be assigned to the intermolecular H-bonds between adjacent subunits holding the polymer together. The loss of intensity of this band may be a result of the fluctuations of the subunits in the polymer, the intermolecular interactions being weaker above the predenaturational transition. Between 80 and 85 °C, a drastic change in the spectra occurs. While the intensities of component bands assigned to secondary structure elements decrease, the maximum band at 1649 cm^{-1} indicates a high content of unordered structures. Remaining contributions at wavenumbers resulting from α-helix and β-sheet show that this denaturation is no total breakdown of the secondary structure; some ordered domains are retained. This might be the reason for the complete reversibility of the denaturation, as can be judged by cooling the denatured sample back to 20 °C, which shows a total renaturation of the secondary structure.

CONCLUDING REMARKS

The thermodynamic parameters and the secondary structure contents of the four bacterial adhesins K88ab, AFA-1, CFA-1, and NFA-1 were obtained for their polymeric forms and, when possible, for the monomeric subunits. All of these highly stable proteins reveal a high level of β-sheet structure. To our knowledge, we are the first to estimate the secondary structure content in a native aggregated form by infrared spectroscopy. These results obtained by IR spectroscopy are not trivial and imply that the protein subunits have to be loosely packed, for example, in a chainlike arrangement held together by hydrophobic interactions (K88ab, AFA-1, CFA-1) or by hydrogen bonding (NFA-1). Unpublished results of proteins in a tightly packed arrangement (e.g., IR investigations of tobacco mosaic virus coat protein, performed in our laboratory) indicate that the interpretation of the infrared data with regard to the secondary structure can be misleading. In this case, the results obtained by interpretation of the IR spectra did not fit to the results obtained by X-ray analysis. While the secondary structure of the oligomeric TMV coat protein was in a good agreement with the X-ray data, the polymeric form showed an apparent structural alteration resulting in an unacceptable high amount of β-sheets and too low an amount of α-helix compared to the X-ray data. However, on condition that other techniques like electron microscopy or light scattering reveal a loose packing of the protein subunits, infrared spectroscopy seems to be well suited to determine the secondary structure of these protein aggregates with high molecular weight, even if the monomeric subunits are not available.

ACKNOWLEDGMENT

Bacterial strains were a gift of Professor Klaus Jann, Max-Planck-Institut für Immunbiologie, Freiburg, Germany. We thank Monika Held (MPI für Immunbiologie) for performing the hemagglutination studies. Ulrike Kühlmann, Michael Bechtold, and Ursula Friedrich are thanked for their technical assistance.

REFERENCES

Ahrends, R. (1991) Ph.D. Thesis, University of Freiburg.
Atanasow, B. P., Derzhanski, A., & Georgieva, A. (1968) *Biochim. Biophys. Acta 160*, 255.
Byler, D. M., & Susi, H. (1986) *Biopolymers 25*, 469.
Clark, A. H., Saunderson, D. H. P., & Suggett, A. (1981) *Int. J. Pept. Protein Res. 17*, 353.
Dousseau, F., & Pézolet, M. (1990) *Biochemistry 29*, 8771.
Duguid, J. P., Smith, H. W., Dempster, J., & Edwards, P. N. (1955) *J. Pathol. Bacteriol. 70*, 335.
Evans, D. G., Silver, R. P., Evans, D. J., Chase, D. G., & Gorbach, S. L. (1975) *Infect. Immunol. 12*, 656.
Evans, D. G., Evans, D. J., Jr., & Tijon, W. (1977) *Infect. Immunol. 25*, 738.
Fabian, H., Choo, L. P., Szendrei, G. I., Jackson, M., Halliday, W. C., Otvos, L., Jr., & Mantsch, H. H. (1993) *Appl. Spectrosc. 47*, 1513.
Fredericks, P. M., Lee, J. B., Osborn, P. R., & Swinckels, D. A. J. (1985) *Appl. Spectrosc. 39*, 311.
Freire, E., & Biltonen, R. L. (1978) *Biopolymers 17*, 463.
Gill, S. C., & von Hippel, P. H. (1989) *Anal. Biochem. 182*, 319.
Jackson, M., Haris, P. I., & Chapman, D. (1991) *Biochemistry 30*, 9681.
Jaenicke, R. (1988) *Forum Mikrobiol. 11*, 435.
Jann, K. & Hoschützky, H. (1990) *Curr. Top. Microbiol. Immunol. 151*, 55.
Kato, K., Matsui, T., & Tanaka, S. (1987) *Appl. Spectrosc. 41*, 861.
Kim, Y. D., & Lumry, R. (1971) *J. Am. Chem. Soc. 93*, 1003.
Klemm, P. (1981) *Eur. J. Biochem. 117*, 617.
Knörle, R., Schnierle, P., Koch, A., Buchholz, N., Hering, F., Seiler, H., Ackermann, Th., & Rutishauser, G. (1994) *Clin. Chem. 40*, 1739.
Labigne-Roussel, A. F., Schmidt, A., Walz, W., & Falkow, S. (1985) *J. Bacteriol. 162*, 1285.
Lee, D. C., Haris, P. I., Chapman, D., & Mitchell, R. C. (1990) *Biochemistry 29*, 9185.
Levitt, M., & Greer, J. (1977) *J. Mol. Biol. 114*, 181.
Loeb, T., & Zinder, N. D. (1961) *Proc. Natl. Acad. Sci. U.S.A. 47*, 282.
Matheson, R. R., Dugas, H., & Scheraga, H. A. (1977) *Biochem. Biophys. Res. Commun. 74*, 869.
Privalov, P. L. (1979) *Adv. Protein Chem. 33*, 167.
Privalov, P. L. (1980) *Pure Appl. Chem. 52*, 479.
Privalov, P. L., & Kechinashvili, N. N. (1974) *J. Mol. Biol. 86*, 665.
Singh, B. R., Fuller, M. P., & Schiavo, G. (1990) *Biophys. Chem. 46*, 195.
Smith, P. K., Krohn, R. I., Hermanson, G. T., Mallia, A. K., Gartner, F. H., Provenzano, M. D., Fujimoto, E. K., Goeke, N. M., Olson, B. J., & Klenk, D. C. (1985) *Anal. Biochem. 150*, 76.
Surewicz, W. K., & Mantsch, H. H. (1988) *Biochim. Biophys. Acta 952*, 115.
Surewicz, W. K., Szabo, A. G., & Mantsch, H. H. (1987) *Eur. J. Biochem. 167*, 519.
Surewicz, W. K., Mantsch, H. H., & Chapman, D. (1993) *Biochemistry 32*, 389.

BI9502351